

## NEW LIGHT SYNTHESIS AND SPECTRUM SYNTHESIS CONSTRAINTS ON A MODEL FOR $\beta$ LYRAE

A. P. LINNELL,<sup>1</sup> I. HUBENY,<sup>2</sup> AND P. HARMANEC<sup>3</sup>

Received 1998 April 3; accepted 1998 July 14

### ABSTRACT

A suite of programs that calculates both synthetic light curves and synthetic spectra for a binary system with an optically thick accretion disk has been applied for the first time to  $\beta$  Lyrae A. Our results demonstrate that the standard accretion disk model by Hubeny & Plavec shows significant residuals from observations, both photometric and spectroscopic, and that no changes in adjustable parameters are able to remove the residuals. The basic problem is that the Hubeny & Plavec model requires a small visible segment of the hot star at the center of the accretion disk and this requirement conflicts with the photometric evidence. As an alternative, we investigate standard accretion disk models in which the central star is hidden from view. We find that no model of this type can satisfy either the observed photometry or the *IUE* spectra. To resolve this impasse, we suggest the presence of a light-scattering region above the accretion disk faces, which scatters light from the central star into the line of sight and provides the high- $T_{\text{eff}}$  radiation component required by both the light curves and the observed spectra. This source of radiation is very likely related to the jets proposed by Harmanec et al. and Hoffman et al. We calculate the location of stream impact on the accretion disk rim. Observations show no detectable photometric signature of a rim bright spot. We suggest that the liberated kinetic energy is spread over a region sufficiently large and at a sufficient optical depth to suppress appearance of a bright spot. A slight asymmetry of primary minimum may indicate swelling of the accretion disk rim downstream from the stream impact point, with an attendant slight increase in obscuration of the background light sources.

*Subject headings:* accretion: accretion disks — binaries: close — binaries: eclipsing — stars: individual ( $\beta$  Lyrae)

### 1. INTRODUCTION

The eclipsing binary  $\beta$  Lyrae A (HR 7106) (hereafter  $\beta$  Lyrae) is one of the most extensively studied of all binary systems. Reviews of the literature are in Sahade (1980) and Harmanec et al. (1996, hereafter HMB96). The  $\beta$  Lyrae system consists of a B6–8 II star that is transferring mass to a more massive star, which is very probably surrounded by a thick accretion disk (Huang 1963). A discussion of this model is in Wilson (1974), and detailed application to an accretion disk model is in a paper by Hubeny & Plavec (1991, hereafter HP). The mass-losing star fills its Roche lobe, it is larger than the mass-gaining star, and primary eclipse in *UBV* corresponds to eclipse of the mass loser, the primary component. The system shows strong emission lines.

The only previous successful simulation of observed  $\beta$  Lyrae light curves has been in the study by Wilson & Lapasset (1981, hereafter WL). WL modeled the secondary component as a greatly flattened object, essentially an oblate spheroid (Wilson 1974). A polar temperature of 15,000 K was required to fit the *UBV* and *OAO 2* light curves. The photospheric temperature profile followed an arbitrary law. WL treated the relative monochromatic luminosities as free parameters for each light curve separately. As HP discuss, the WL model cannot represent sub-

sequently observed UV spectra. Models of accretion disks have been developed largely since the WL study and an accretion disk model now should supplant the WL model. Hubeny, Harmanec, & Shore (1994) further discuss model alternatives.

Until recently no suitable light synthesis and spectrum synthesis program has existed to simulate a binary system including an optically thick accretion disk. Zhang, Robinson, & Nather (1986, see also Zhang & Robinson 1987) developed a light synthesis code for cataclysmic variables with an optically thick accretion disk. In their model the accretion disk rim is thin enough to be neglected as a source of radiation, except for a bright spot. Zola (1996, and references therein; see also Zola, Hall, & Henry 1994) modified the Wilson-Devinney (1971) program to include an optically thick accretion disk. Neither of these two programs calculates synthetic spectra.

Linnell & Hubeny (1996a, hereafter LH) have developed a set of spectrum synthesis and light synthesis programs for binary stars with optically thick accretion disks. We call this set of programs the BINSYN suite. BINSYN thus produces and combines separate synthetic spectra of the two stars, the accretion disk face and the accretion disk rim. BINSYN applies the standard accretion disk model (Frank, King, & Raine 1992, hereafter FKR). In the original version the accretion disk rim was represented by a cylindrical section. That representation has now been replaced by a theoretically preferable half-toroid. BINSYN allows us to produce both theoretical light curves for a specified set of effective wavelengths and synthetic spectra at specified orbital longitudes and over specified wavelength intervals, all on a common, physically self-consistent basis. The suite has recently been augmented to include simulation of a rim bright spot. BINSYN also now includes a solution for the

<sup>1</sup> Department of Physics and Astronomy, Michigan State University, East Lansing, MI 48824; Visiting Scholar, Astronomy Department, University of Washington, Seattle, WA 98195; linnell@pa.msu.edu (address inquiries here).

<sup>2</sup> AURA/NOAO NASA Goddard Space Flight Center, Code 681, Greenbelt, MD 20771; hubeny@stars.gsfc.nasa.gov.

<sup>3</sup> Astronomical Institute, Academy of Sciences, 251 65 Ondřejov, Bohemia, Czech Republic; hec@sunstel.asu.cas.cz.

trajectory of a mass transfer stream (Lubow & Shu 1975), simulation of the boundary layer, and modeling of the reflection effect on the accretion disk rim of radiation from the component filling its Roche lobe.

We have used BINSYN to produce synthetic light curves and synthetic spectra, using the HP and an alternative model, for comparison with available  $\beta$  Lyrae observational data. We discuss the comparisons in the following sections. As a matter of terminology, “secondary minimum” always refers to the phase 0.5 eclipse for  $V$  observations and “primary minimum” to the phase 0.0 eclipse, irrespective of which eclipse is deeper at the wavelength under study.

## 2. KNOWN SYSTEM CONSTRAINTS

What system parameters are reasonably well known? The recent work by Harmanec & Scholz (1993, hereafter HS) provides a secure value (0.223) for the mass ratio, which is specified as the mass of the star eclipsed at primary minimum divided by the mass of the star eclipsed at secondary minimum. The primary component (mass loser)  $T_{\text{eff}}$  is known from the study by Balachandran, Lambert, & Tomkin (1986). From period change data it follows that the primary is losing mass to the secondary and so fills its Roche lobe. Evolutionary studies (De Greve & Linnell 1994) support this interpretation. The HP study, as well as the light-curve analysis in WL, shows that the orbital inclination must be in the vicinity of  $i = 83^\circ$ . The system parallax from the *Hipparcos* catalog (Perryman et al. 1997) is 3.70 mas, giving a distance of 270 pc, and replacing the value of 370 pc by Dobias & Plavec (1985). (This topic is the subject of further discussion in § 3.)

Polidan (1989) and others have suggested that the secondary component may be a collapsed object, which, for the known mass, would be a black hole. X-rays from  $\beta$  Lyrae have been detected but the flux is typical for an early B-type star (Berghöfer & Schmitt 1994), not a black hole source. The secondary component mass rules out the possibility that it is either a neutron star or a white dwarf. It is likely that the secondary is rotating rapidly, possibly nearly at critical rotation (Wilson 1981; HP). This condition has a negligible effect on the light curves, apart from any possible boundary layer effect, for the following reason. In the Roche model there is zero polar compression of a critically rotating star; the equator expands by a factor 1.5. For a synchronously rotating polytrope of index  $n = 3.0$ , at critical rotation, the polar compression is relatively minor (Linnell 1981, Table VII) and the ratio of equatorial to polar radius is close to 1.5. To have any appreciable effect on the light curves, the secondary component radius, polar or equatorial, would have to change by a factor between 5.0 and 10.0. We adopted synchronous rotation for both components for the tests reported in this paper.

HP point out that “in typical Algol-like semidetached systems, the gainer looks like a normal main-sequence star.” We adopt a main-sequence star status for the secondary component. Also adopting  $i = 83^\circ$ , the  $\mathcal{M} \sin^3 i$  data from HS, and the HS value  $q = 0.223$ , we find that the primary component mass is  $2.9 \mathcal{M}_\odot$  and the secondary component mass is  $13.1 \mathcal{M}_\odot$ . HP quote data for V453 Cygni and CW Cephei, whose masses bracket the secondary component mass. The  $T_{\text{eff}}$  value for both quoted stars is 29,000 K. The tabulation by Harmanec (1988) provides a radius of  $6 R_\odot$  for a  $13 \mathcal{M}_\odot$  star. We adopt these values for the  $T_{\text{eff}}$  and radius of the secondary component.

HP adopt an accretion disk radius of  $25 R_\odot$ . This value is close to the tidal cutoff radius (Paczynski 1977). Harmanec (1992) made estimates of system parameters from different geometrical considerations and also arrived at a radius of  $6 R_\odot$  for the secondary star and a radius of order  $25 R_\odot$  for the accretion disk. The radius of the accretion disk must be an adjustable parameter to achieve a good fit to the photometric data. Our model uses the same accretion disk radius to calculate theoretical light curves at all wavelengths of observation.

The mass transfer rate,  $\dot{\mathcal{M}}$ , is not well established. The reason for this is that it can only be measured indirectly from the observed properties of the system. First, one may use the observed increase of the orbital period. This determination, however, is hampered by our ignorance of the degree to which the mass transfer process is conservative. Assuming the mass transfer to be conservative (i.e., all mass transferred from the primary component is eventually captured by the secondary star), HS determined a mass transfer rate of about  $20 \times 10^{-6} \mathcal{M}_\odot \text{ yr}^{-1}$  from the observed period increase rate of  $18.9 \text{ s yr}^{-1}$ . Another possibility is to use evolutionary considerations; De Greve & Linnell (1994) found a current value of  $28 \times 10^{-6} \mathcal{M}_\odot \text{ yr}^{-1}$ . Note that the evolutionary calculation finds that the mass transfer is not conservative. Finally, the mass transfer rate can be determined from spectrophotometric properties of the accretion disk around the mass-gaining star, which is the standard procedure used for the cataclysmic variable (CV) systems. However, applying this approach for  $\beta$  Lyrae is very difficult. First, since we see the system almost edge-on, the disk face is largely or completely hidden from view (see below). The most visible part of the disk is the disk rim, which, unfortunately, is the least understood region of accretion disks in close binary systems. The basic physical problem is that several fundamental assumptions that are the building blocks of the standard model fail in the disk rim layers. Among them, the most important one is the assumption of Keplerian rotation. As discussed by HP and verified by detailed two-dimensional and three-dimensional hydrodynamic simulations (Lin & Pringle 1976; Hirose, Osaki, & Mineshige 1991; Osaki, Hirose, & Ichikawa 1993; Rózycka & Schwarzenberg-Czerny 1987; Armitage & Livio 1996, 1998; Blondin 1997), the tidal torques and the interaction of the disk rim with the stream coming from the mass-losing component will lead to departures from Keplerian rotation, as well as to departures from a simple homogeneous structure.

To deal with the problem of the rim in the absence of detailed hydrodynamic simulations, HP devised a crude model of the disk rim that was meant to provide a zero-order estimate of (1) the disk rim shape and (2) the rim  $T_{\text{eff}}$ . In the HP theory the rim  $T_{\text{eff}}$  is equal to that of the last tidally stable ring in the Keplerian disk. That ring is at a distance of approximately 0.85 of the Roche lobe of the mass-gaining star. Therefore, the rim  $T_{\text{eff}}$  is a unique function of  $\mathcal{M}_s$ ,  $R_s$ , and  $\dot{\mathcal{M}}$ . HP showed that the observed  $\beta$  Lyrae properties are roughly consistent with a rim  $T_{\text{eff}}$  corresponding to  $\dot{\mathcal{M}} = 100 \times 10^{-6} \mathcal{M}_\odot \text{ yr}^{-1}$ . This value cannot be taken as a *determination* of  $\dot{\mathcal{M}}$ , but rather evidence that the  $\dot{\mathcal{M}}$  should be high. We stress that the HP theory considers that the energy generated in the rim arises solely from viscous dissipation. In reality, there are other sources of mechanical energy, so the rim  $T_{\text{eff}}$  would likely be higher than that indicated by the HP theory, or, alternative-

TABLE 2  
CALCULATED PARAMETERS, HP MODEL

Parameter	Value	Parameter	Value
$\mathcal{M}_s$ ( $\mathcal{M}_\odot$ ).....	13.05	$A$ ( $R_\odot$ ).....	58.35
$\mathcal{M}_D$ ( $10^{-6} \mathcal{M}_\odot$ ).....	23.	$T_{r,eq}$ (K).....	6642
$R_p$ (pole) ( $R_\odot$ ).....	14.02	$T_p$ (pole) (K).....	13300
$R_p$ (point) ( $R_\odot$ ).....	20.50	$T_p$ (point) (K).....	6477
$R_p$ (side) ( $R_\odot$ ).....	14.59	$T_p$ (side) (K).....	12789
$R_p$ (back) ( $R_\odot$ ).....	16.48	$T_p$ (back) (K).....	11205
$R_s$ (pole) ( $R_\odot$ ).....	5.98	$T_s$ (pole) (K).....	29000
$R_s$ (point) ( $R_\odot$ ).....	5.99	$T_s$ (point) (K).....	28970
$R_s$ (side) ( $R_\odot$ ).....	5.99	$T_s$ (side) (K).....	28981
$R_s$ (back) ( $R_\odot$ ).....	5.99	$T_s$ (back) (K).....	28971

ly, an empirically determined rim  $T_{\text{eff}}$  would associate with a lower  $\mathcal{M}$  than dictated by the HP theory.

$\mathcal{M}$  only affects the calculated light curves by setting the temperature profile on the accretion disk face and the rim temperature.

### 3. LIGHT SYNTHESIS LIGHT CURVES ON THE HUBENY-PLAVEC MODEL

Our *UBV* observational data are from HMB96. The *OA0 2* observational data are from Kondo et al. (1994). Table 1 lists the input parameters to the BINSYN routines. The parameter symbols have their standard meanings. The subscripts  $p, s$  denote the primary component and the secondary component, respectively. The quantities  $F_p$  and  $F_s$  are rotation parameters, defined to be the rotation rate in units of the synchronous rate.  $A_{p,s,\text{rim}}$  are bolometric albedos.  $g_{p,s}$  are gravity brightening exponents.  $R_A$  is the orbital plane radius of the accretion disk, and  $H$  is the semithickness of the accretion disk rim measured at the inner edge of the toroidal cross section. Some derived system parameters are in Table 2. The calculated disk mass,  $\mathcal{M}_D$ , is from HH. The quantity  $T_{r,eq}$  is the rim  $T_{\text{eff}}$  value in the rim equatorial plane, not including irradiative heating by the primary component.

We represented the photosphere of each star with a grid of 1970 points. The representation of the accretion disk face used 33 rings with 91 division points on each ring. There were 91 division points on each of the nine rim grid circles. As described in LH, a visibility key attached to each grid point on each object receives an assigned value for each fiducial orbital longitude. The visibility keys determine whether the associated surface element is visible to the observer and permit calculation of the integrated flux from the system, at the specified wavelength. The calculations reported in this paper used 81 fiducial orbital longitudes.

TABLE 1  
INPUT PARAMETERS, HP MODEL

Parameter	Value	Parameter	Value
Period (days).....	12.9335	$i$ (deg).....	83.0
$q$ .....	0.223	$T_{\text{eff},p}$ (K).....	13300
$\mathcal{M}_{\odot,p}$ .....	2.91	$T_{\text{eff},s}$ (K).....	29000
$\Omega_p$ .....	8.50	$\mathcal{M}$ ( $10^{-6} \mathcal{M}_\odot \text{ yr}^{-1}$ ).....	100
$\Omega_s$ .....	43.0	$R_A$ ( $R_\odot$ ).....	30.0
$F_p$ .....	1.0	$H$ ( $R_\odot$ ).....	5.99
$F_s$ .....	1.0	$A_{\text{rim}}$ .....	0.5
$A_p$ .....	1.0	$g_p$ .....	0.25
$A_s$ .....	1.0	$g_s$ .....	0.25

Theoretical light values at individual orbital phases of observation were calculated with Newton's method of interpolation using second differences. The program separates the light curve into appropriate phase ranges to avoid interpolation over points where there is a discontinuous first derivative of the system light with respect to orbital phase.

The  $T_{\text{eff}}$  values for the accretion disk face rings are calculated in BINSYN using the standard theory (HP, eq. [2]). The rim  $T_{\text{eff}}$  is from HP, equations (18) and (19). (Note the discussion in § 2 above.)

The number of simulations involved in our exploration of parameter space made it necessary to approximate the radiation characteristics of the system components. Normally, the BINSYN suite produces light curves by first calculating composite system synthetic spectra for a large number of fiducial orbital longitudes. It then integrates the product of each synthetic spectrum and one or more standard response functions, in analogy to the procedure of Buser & Kurucz (1992). Interpolation among the products then produces light curves for comparison with observation (Linnell, Hubeny, & Lacy 1996b; Linnell et al. 1998). This procedure would have been prohibitively time consuming for the number of simulations required in our study. A blackbody approximation at the  $T_{\text{eff}}$  of each grid point is an adequate approximation for survey purposes. BINSYN also requires limb-darkening values for each grid point. We used the coefficients of Wade & Rucinski (1985), interpolated automatically to the local values of  $T_{\text{eff}}$  and  $\log g$ . The differences between our light curves calculated by this procedure and by the more physically accurate procedure would be a few hundredths of a magnitude. The photometric effects on which we base our argument are far larger.

Appropriate values for the bolometric albedos require some consideration. BINSYN does not currently treat irradiation of the central star by the faces of the accretion disk. Accordingly we have set the bolometric albedo of the secondary component to 0.0. The accretion disk may partially shadow the mass loser from irradiation by the mass gainer by an amount that depends on the thickness of the rim. In our case the rim is thick enough to shadow the primary nearly completely. The rim radiation also illuminates the primary, and with a color temperature that differs greatly from that of the secondary component. On the HP model, the extreme polar regions of the primary would be illuminated by the secondary. We argue below that no part of the primary receives undiluted direct radiation from the secondary, and so this illumination is unimportant in our representation. As a separate issue, since the primary fills its Roche lobe, normal gravity brightening for a radiative envelope would imply, at the L1 point where the gravity becomes 0.0, a  $T_{\text{eff}}$  value of 0 K (Linnell 1984, eq. [31]). The gravity brightening model must break down in the L1 region. Because of these considerations, we have arbitrarily used a bolometric albedo of 0.1 for the primary component and have assumed illumination of it by the secondary as if no accretion disk were present. The resulting temperature profile is in Table 2 and must be closer to physical reality than if the bolometric albedo were set to 0.0. The effect on the theoretical light curves is negligible.

In our model, the accretion disk rim is thick and is proximate to a B8 star. There could be a nonnegligible reflection effect on the rim from the incident radiation originating on the primary component. Accordingly, BINSYN has been enhanced to include a theory of irradiation of the accretion

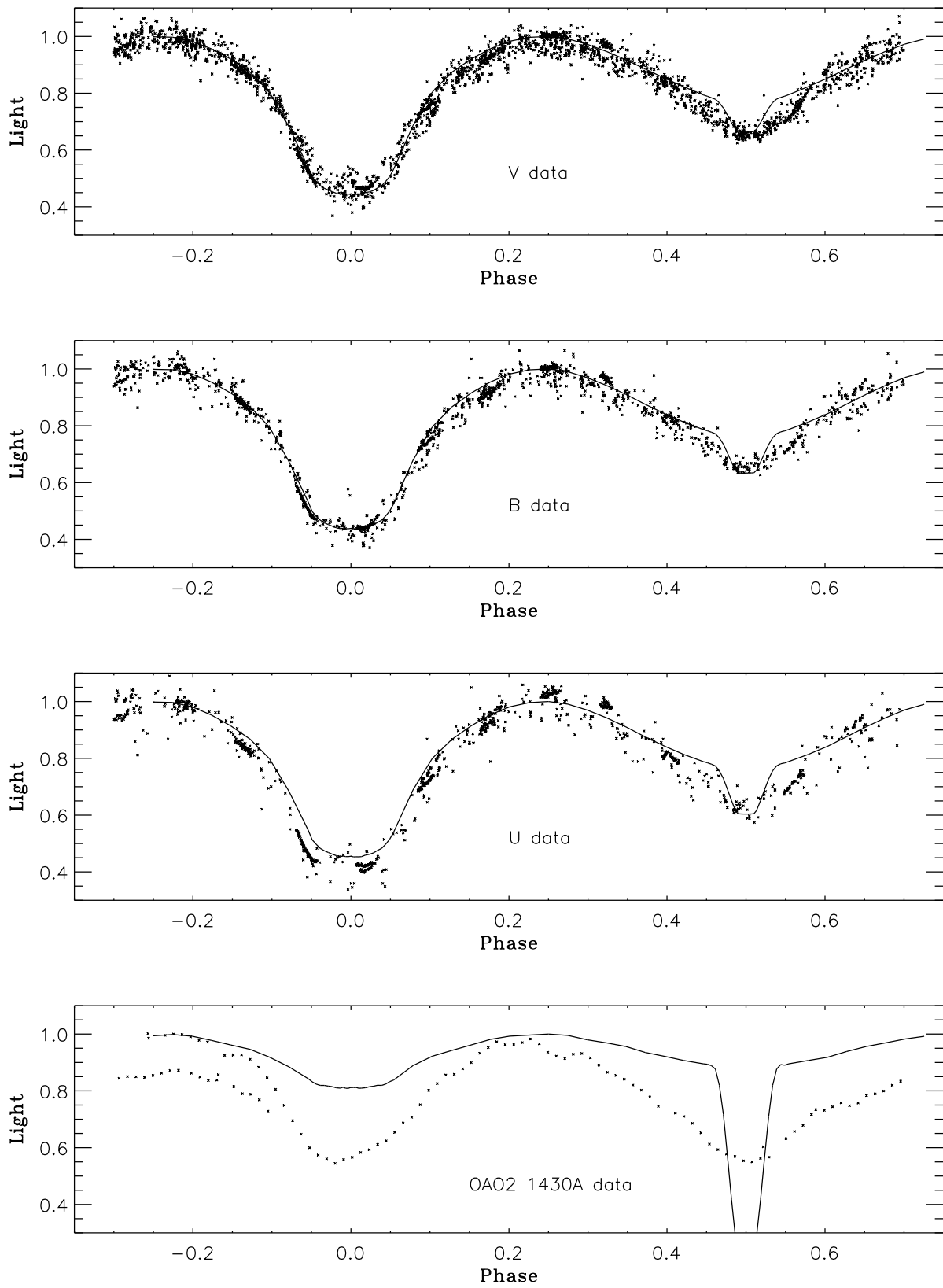


FIG. 1.—Comparison of theoretical and observed light curves on the HP model. Note the presence of a stellar eclipse at the center of secondary minimum in the theoretical light curves. That feature is not present in the observed light curves. Instead, the observed light curves show an eclipse of a more extended luminous region.

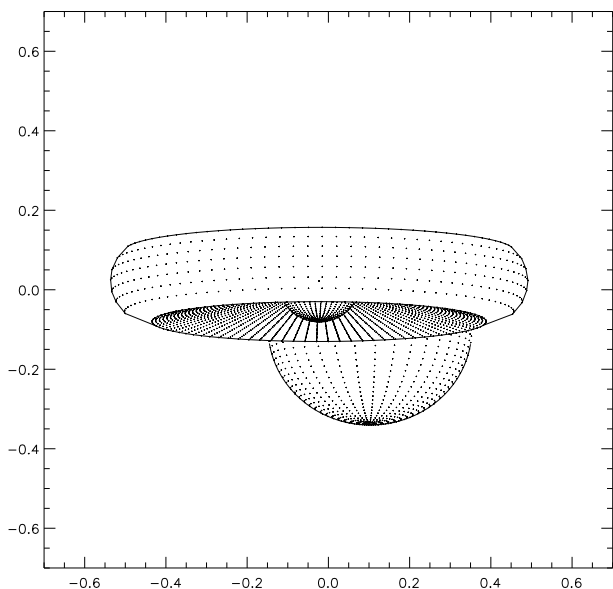


FIG. 2.—View of the HP model projected on the plane of the sky at orbital phase 0.0158. This phase is the same as that of an *IUE* observed spectrum. Note the visibility of a small segment of the secondary component at the center of the accretion disk. See text for a discussion of the accretion disk rim.

disk rim by a distorted companion with nonuniform photospheric  $T_{\text{eff}}$ , radiating as a blackbody with assignable bolometric limb darkening, and with a specified bolometric albedo for the accretion disk rim. The situation in this instance is complicated by the fact that the primary fills its Roche lobe and has a radiative envelope. The substellar equatorial rim point faces a primary component that, as just discussed, has a  $T_{\text{eff}}$  value (in the absence of irradiation) of 0 K at the primary's closest point to the rim. Moving either in azimuth or in latitude on the rim exposes the rim to radiating regions of rapidly increasing temperature on the primary component. The effect on the light curves is negligible, as discussed below.

The only Table 1 parameters subject to adjustment, in a fit to the photometric and spectroscopic data, are  $i$ ,  $\mathcal{M}$ ,  $R_A$ , and  $H$ .

With the parameters of Table 1, BINSYN produced the light curves of Figure 1, shown superposed on the *UBV* light curves and *OAO 2* data. Our parameters differ very slightly from HP and have been adjusted to produce the best possible fit to the *V* light curve. BINSYN used a fixed set of system parameters to calculate the light curves at their various effective wavelengths. For simplicity we call this the HP model.

The fit to primary minimum in *V* and *B* is quite good, and also the fit to the depth of secondary minimum. The fit to the *U* light curve is not nearly so good. We emphasize again that the simulation has used a standard model accretion disk, and that the disk resides entirely within its Roche lobe. A simulation of this type has not been done before, and we consider our result to be an important advance.

The *Hipparcos* parallax of  $\beta$  Lyr,  $\pi = 0.00370 \pm 0.00052$ , gives a chance to carry out an independent check of the consistency of the adopted basic physical elements of the binary and our light-curve solutions. One can estimate the total brightness of the binary at light maxima to be  $V_{p+s} = 3.35$  mag (see Fig. 2 of Harmanec et al. 1996). For  $E(B-V) = 0.04$  mag, this implies a dereddened total *V*

magnitude of 3.23 mag. For the *Hipparcos* parallax, this gives  $M_{V(p+s)} = -3.93$  mag, with the range from  $-3.64$  mag to  $-4.26$  mag due to the error of the parallax. Adopting the flux ratio in the *V* band between the primary and secondary,  $F_p/F_s = 5.19$  from the light-curve solution at orbital phase  $\pi/2$  (the ellipticity effect of the primary component is substantial), one obtains  $M_{V,p} = -3.74$  mag and  $M_{V,s} = -1.95$  mag. For a bolometric correction of 1.0 mag and  $T_{\text{eff}} = 13,300$  K, one obtains  $R_p = 14.86 R_{\odot}$  (range from 13.00 to 17.30  $R_{\odot}$ ). This is in very good agreement with the Roche lobe radius of the primary that follows from the orbital elements of HS: 14.6  $R_{\odot}$ . (See Table 2 also.)

A separate result also is apparent. *The central star in the accretion disk cannot directly contribute to the system light.* The modeled eclipse of the central star produces a narrow stellar eclipse in secondary minimum, with a width of 0.05 orbital period, that is ruled out observationally. This point was originally made by Wilson (1974). See WL also. This stellar eclipse, for the adopted  $T_{\text{eff}}$  of the secondary, becomes deeper at shorter (UV) wavelengths where the discrepancies with observation become extreme (Fig. 1, bottom). The character of the theoretical light curve does not change with variation in either the mass ratio or  $i$ . We have run many simulations with a wide variety of system parameters and find no combination of adjustable parameters, together with the fixed known parameters, that can satisfactorily represent the observed light curves. Since our results are clear from the direct light-curve plots, we omit any residuals plots.

A projection view of the system at orbital phase 0.0158 is in Figure 2. The rim has been represented with nine division circles on the toroidal boundary. The upper division circle lies below the observer's horizon. More than nine division circles would provide intermediate divisions between the topmost one now visible (the second division circle) and the first (hidden) circle. This would produce a more symmetric appearance for the accretion disk, and it would slightly raise the visible upper boundary, but it would change the light curves by a nearly negligible amount. Unfortunately, the present software has a limit of nine division circles on the accretion disk rim and an appreciable effort will be needed to increase that limit.

We do not discuss the infrared observations of  $\beta$  Lyrae (Jameson & Longmore 1976, hereafter JL). Observations show that the secondary minimum becomes deeper than primary minimum at long wavelengths. JL conclude that the observations can be explained by a plasma cloud around the secondary component. We return to this point later in this paper.

#### 4. SPECTRUM SYNTHESIS ON THE HUBENY-PLAVEC MODEL

Figure 3 is at the orbital phase of the *IUE* spectra SWP 35707 and LWP 15148. In calculating the phases of the *IUE* spectra we used the ephemeris in HS. The two *IUE* spectra were merged and extinction corrected with the IUESIPS UNRED utility, with the CCM option, and using  $E(B-V) = 0.03$  mag. Dobias & Plavec (1985) determined a value  $E(B-V) = 0.04$  mag and a distance to  $\beta$  Lyrae B of 370 pc. The *Hipparcos* value, discussed in § 2, is 270 pc. Consequently we have arbitrarily reduced the reddening value to  $E(B-V) = 0.03$  mag. We have redone the unreddening for  $E(B-V) = 0.04$  mag. The two unreddened spectra differ by a negligible amount.

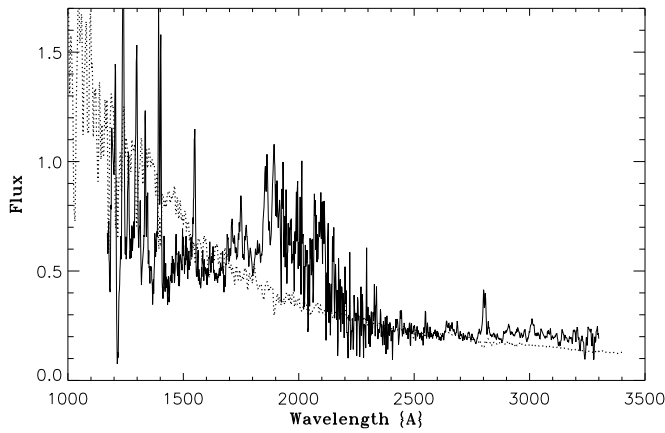


FIG. 3.—Comparison of the observed *IUE* spectrum during primary minimum, at the orbital phase of Fig. 2, and a synthetic spectrum on the HP model. The observed (*IUE*) spectrum is the continuous line. The synthetic spectrum is the dotted line. The continuum fits fairly well, except shortward of 1500 Å. See text for discussion.

Details of our procedure for calculating synthetic spectra are in LH. We calculate a number of synthetic spectra for specific values of  $T_{\text{eff}}$  and  $\log g$  to associate with each system object (primary, secondary, accretion disk face, accretion disk rim). These spectra bracket the extreme values of  $T_{\text{eff}}$  on the object in question and are sufficient in number to permit linear interpolation to the local  $T_{\text{eff}}$  values on all the grid points of that object. We neglect variation in  $\log g$ , although our software permits us to take it into account. The source synthetic spectra, calculated with program SYNSPEC, include specific intensities for a range of zenith distances at each tabular wavelength. By interpolation, these data permit us to calculate the contribution of each element of area on each system component to the system spectrum. For the primary component we used four source synthetic spectra, calculated using Kurucz solar composition model atmospheres of  $T_{\text{eff}} = 4000, 11,000, 12,000,$  and  $13,000$  K,  $\log g = 4.0$ . We used a single Kurucz solar composition model atmosphere of  $T_{\text{eff}} = 30,000$  K for the synthetic spectrum representing the secondary star. For the rim we calculated synthetic spectra from Kurucz solar composition model atmospheres of  $T_{\text{eff}} = 4000$  and  $6500$  K,  $\log g = 4.0$ . We used the program TLUSDISK to calculate synthetic spectra for the accretion disk face of  $T_{\text{eff}} = 11,000, 12,000,$  and  $13,000$  K, solar composition. To these we added synthetic spectra calculated by SYNSPEC with Kurucz solar composition model atmospheres of  $T_{\text{eff}} = 9000$  and  $10,000$  K,  $\log g = 4.0$ , giving a total of five synthetic spectra to represent the accretion disk face.

A comparison of the unreddened *IUE* spectrum and a synthetic spectrum on the HP model is in Figure 3. In agreement with the HP study, the theoretical continuum fits the observed continuum reasonably well. The theoretical continuum is too bright shortward of about 1500 Å. The emission bump is prominent; its presence makes it difficult to estimate the strength of the underlying continuum.

We conclude that the HP model, although meeting its original objective of modeling the  $\beta$  Lyrae continuum within the framework of an accretion disk system, cannot be the correct model. The basic problem is that the visible small segment of the central star, needed in the HP model to provide the spectral continuum component of high  $T_{\text{eff}}$ , produces a stellar eclipse during secondary minimum that is

inconsistent with observations. The spectrum of the small central star segment, with its absorption lines appropriate to 29,000 K, dominates the far-UV system spectrum and produces a system spectrum for Ly $\alpha$  that differs greatly from that observed. Geocoronal Ly $\alpha$  emission is unimportant. Having shown that the HP model, with its *visible* segment of the central star, conflicts with observational data, we inquire whether a viable standard accretion disk model exists in which the central star is completely *hidden*.

## 5. AN ALTERNATIVE ACCRETION DISK MODEL

Our aim is to search for a standard model accretion disk system with a rim sufficiently thick completely to hide the central star and yet to provide an acceptable fit to the observed light curves. A separate requirement would be an acceptable fit to the continuum spectrum. Extensive experiment isolated a region of parameter space that permits a fairly good fit to the *UBV* light curves. The system parameters finally chosen are in Table 3. With the exception of the parameters in the first two rows of Table 3, the input parameters are the same as for the HP model, Table 1. Thus the alternative model preserves consistency with known system parameters (§ 2).

By adopting a sufficiently thick accretion disk rim it is possible to hide the central star entirely. This procedure entails loss of the high- $T_{\text{eff}}$  contribution of the central star and initially produces a secondary minimum that is too shallow. Raising the  $T_{\text{eff}}$  of the rim compensates, but the brighter rim now contributes additional light at primary minimum and outside eclipse. This renormalizes system light outside eclipse and so tends to make primary minimum shallower. On the other hand, the greater rim thickness eclipses more of the primary component, tending to deepen primary minimum. Within limits, changing the orbital inclination can vary the depth of primary minimum without appreciably affecting the depth of secondary minimum. We take the rim  $T_{\text{eff}}$  to be a free parameter, an assignment justified by our discussion in § 2. Within the framework of BINSYN, this is accomplished by making  $\mathcal{M}$  a free parameter and using the HP theory to calculate the corresponding rim  $T_{\text{eff}}$ .

We varied the system parameters empirically to achieve a fit to the light curves. For the adopted value of  $i$ ,  $H$  must be as large as it is to produce a sufficiently deep primary minimum. Also, for the adopted value of  $H$ , the rim  $T_{\text{eff}}$  must be as large as it is to produce a sufficiently deep secondary minimum. The depth of primary minimum does not increase strongly with increasing  $i$ , for  $i = 86^\circ$ , both because

TABLE 3  
PARAMETERS, ALTERNATE MODEL

Parameter	Value	Parameter	Value
$R_A (R_\odot)$ .....	32.0	$i$ (deg) .....	86.0
$H (R_\odot)$ .....	10.0	$\mathcal{M} (10^{-6} \mathcal{M}_\odot \text{ yr}^{-1})$ .....	700
$T_{r,\text{eq}} (\text{K}, 0^\circ)$ .....	11036	$T_{r,\text{eq}} (\text{K}, 40^\circ)$ .....	11002
$T_{r,\text{eq}} (\text{K}, 4^\circ)$ .....	11042	$T_{r,\text{eq}} (\text{K}, 44^\circ)$ .....	10988
$T_{r,\text{eq}} (\text{K}, 8^\circ)$ .....	11055	$T_{r,\text{eq}} (\text{K}, 48^\circ)$ .....	10977
$T_{r,\text{eq}} (\text{K}, 12^\circ)$ .....	11067	$T_{r,\text{eq}} (\text{K}, 52^\circ)$ .....	10968
$T_{r,\text{eq}} (\text{K}, 16^\circ)$ .....	11072	$T_{r,\text{eq}} (\text{K}, 56^\circ)$ .....	10962
$T_{r,\text{eq}} (\text{K}, 20^\circ)$ .....	11070	$T_{r,\text{eq}} (\text{K}, 60^\circ)$ .....	10957
$T_{r,\text{eq}} (\text{K}, 24^\circ)$ .....	11061	$T_{r,\text{eq}} (\text{K}, 64^\circ)$ .....	10955
$T_{r,\text{eq}} (\text{K}, 28^\circ)$ .....	11047	$T_{r,\text{eq}} (\text{K}, 68^\circ)$ .....	10954
$T_{r,\text{eq}} (\text{K}, 32^\circ)$ .....	11032	$T_{r,\text{eq}} (\text{K}, 72^\circ)$ .....	10953
$T_{r,\text{eq}} (\text{K}, 36^\circ)$ .....	11016	$T_{r,\text{eq}} (\text{K}, 180^\circ)$ .....	10953

that value is so close to the limiting  $i = 90^\circ$  and because the (warmer) upper polar region emerges from eclipse as the (cooler, Table 2) near-equatorial regions enter eclipse (Fig. 6). Notice that  $\dot{M}$  in Table 3 is more than an order of magnitude larger than expected from the period change under the assumption of conservative mass transfer. This is a consequence of the requirement for an elevated rim  $T_{\text{eff}}$  and its production by the assumed  $\dot{M}$ .

A limiting case is reached for  $i = 90^\circ$ , with the rim thick enough completely to eclipse the primary component at primary minimum. Preservation of the relative depths of the minima in *UBV* would require a further increase in the rim  $T_{\text{eff}}$  beyond our alternative model, requiring a still larger  $\dot{M}$ . In this limiting case the only objects contributing to the system light are the primary component and the accretion disk rim. In contrast to the WL model, with its hot polar region for the secondary component, the standard model accretion disk rim is nearly isothermal. To make the theoretical secondary minimum in *UBV* shallower than primary minimum, as required by observation, the rim  $T_{\text{eff}}$  must be less than the primary component  $T_{\text{eff}}$ . But with this  $T_{\text{eff}}$  the calculated secondary minimum cannot become deeper than primary minimum at UV wavelengths, in contradiction to observation. Thus the  $i = 90^\circ$  case, with its larger, hotter rim, is excluded.

Returning to the Table 3 case, the rim  $T_{\text{eff}}$  without irradiation required a corresponding bolometric albedo of 1.0, appropriate to a radiative atmosphere. Table 3 lists the  $T_{\text{eff}}$  values for the equatorial profile of the rim at tabular intervals of  $4^\circ$  in the equatorial plane, beginning at the substellar point on the line of centers of the stellar components. The calculated increase in rim  $T_{\text{eff}}$  reaches a maximum of only 120 K (Table 3) and the effect on the theoretical light curves is negligible.

The chosen parameters produced the light curves of Figure 4. Figure 5 shows additional light curves compared with *OAO 2* data. These light curves illustrate two important points.

First, note the reduction in the observed amplitude of light variation, with a minimum amplitude at 1910 Å. It has been suggested that this effect arises from a concentration of emission lines near 2000 Å (Hack 1974; Viotti 1976; Mazzali 1987; Aydin et al. 1988; Mazzali et al. 1992). On this model the emission comes from an extended region of space above and below the accretion disk, and a large part of it remains uneclipsed by the primary component. In their discussion of *Copernicus* data, Hack et al. (1977) state that the measured depth of secondary minimum in continuum light alone is the same, within observational error, as the depth of secondary minimum including emission lines for the wavelength intervals  $\lambda\lambda 2050\text{--}2095$  and  $\lambda\lambda 2580\text{--}2630$ . The attribution of the emission bump to the source of third light, although the most reasonable explanation, is not completely certain. Following WL, we have represented the reduction in eclipse amplitude by adopting appropriate amounts of third light in our light-curve calculations. Specifically, we have adopted fractional third light contributions of 0.10, 0.95, 0.20, and 0.10 at wavelengths 2460, 1910, 1550, and 1430 Å, respectively. The third light contributions are fractions of the total system light at orbital phase 0.25. The light-curve amplitude becomes relatively insensitive to the amount of third light when the third light fraction becomes larger than about 0.50; the value 0.95 at 1910 Å is a low weight determination. None of the other light curves

requires a third light contribution. For comparison, the corresponding values found by WL (solution A) were 0.01, 0.45, 0.06, and 0.00.

Second, even with the artifices of third light and a hot rim, our model fails accurately to represent the observed light curves. The observed light curves show a progressive trend, with secondary minimum becoming equal in depth to primary minimum at 1550 Å and deeper than primary minimum at 1430 Å. The residuals in the present simulation are opposite in character to the residuals in the HP simulation. What the present simulation has lost is the high- $T_{\text{eff}}$  component provided by the hot central star in the HP model. What the present simulation has gained is a good representation of the shapes of the light curves, particularly at secondary minimum. The very roughly comparable depths of primary and secondary minima at all observed wavelengths demonstrates that the average  $T_{\text{eff}}$  values of the eclipsed objects must also be roughly comparable. That is the reason the hot rim model works at all.

The gradual deepening of secondary minimum relative to primary minimum in the observations demonstrates that the  $T_{\text{eff}}$  of a light source missing from our model must be high, comparable with the  $T_{\text{eff}}$  of the central star in the accretion disk. (Note that Aydin et al. 1988 find that secondary minimum already is deeper than primary minimum at 1670 Å, in contrast to the Kondo et al. 1994 *OAO 2* results.) This high- $T_{\text{eff}}$  light component is eclipsed at secondary minimum. Consequently it must differ from the third light component that is not eclipsed. The gradual progressive changes in observed light-curve depths imply that the light source does not originate with emission lines concentrated within short wavelength ranges. The absence, in the observations, of a stellar eclipse at secondary minimum, or anything resembling a stellar eclipse, implies that the high- $T_{\text{eff}}$  source must be more extended, geometrically, than the hidden central star. The requirement that secondary minimum be shallower than primary minimum at all but the shortest observed wavelength prohibits the high- $T_{\text{eff}}$  source from having a higher *surface brightness* than the primary component at those wavelengths. This consideration excludes a stellar photosphere.

Why were WL able to produce a reasonable fit to observed light curves and our simulations have been unsuccessful? First, note that WL fitted each light curve separately, without requiring the radiation characteristic of a given component at one wavelength of observation to have a prescribed connection to the radiation characteristic at another wavelength. (WL did a simultaneous solution for the geometric parameters.) Our simulation has connected the radiation characteristics at all wavelengths to the prescription of the Planck law. Second, the WL model was an ad hoc model in which the  $T_{\text{eff}}$  on the secondary component was a not unreasonable assumed profile, but was not based on a physical theory. We are restricted to a standard model accretion disk, albeit with a rim  $T_{\text{eff}}$  that is a free parameter. The most important difference between the WL model and ours is that the WL model adopts a polar  $T_{\text{eff}}$  that is greater than that of the primary component. It is this feature that permits WL to fit the UV light curves and produce a phase 0.5 minimum that is deeper than the eclipse at phase 0.0. It is precisely this feature of the WL model that is missing from our simulation and is a feature that the standard model cannot provide if the central star is completely hidden from view.

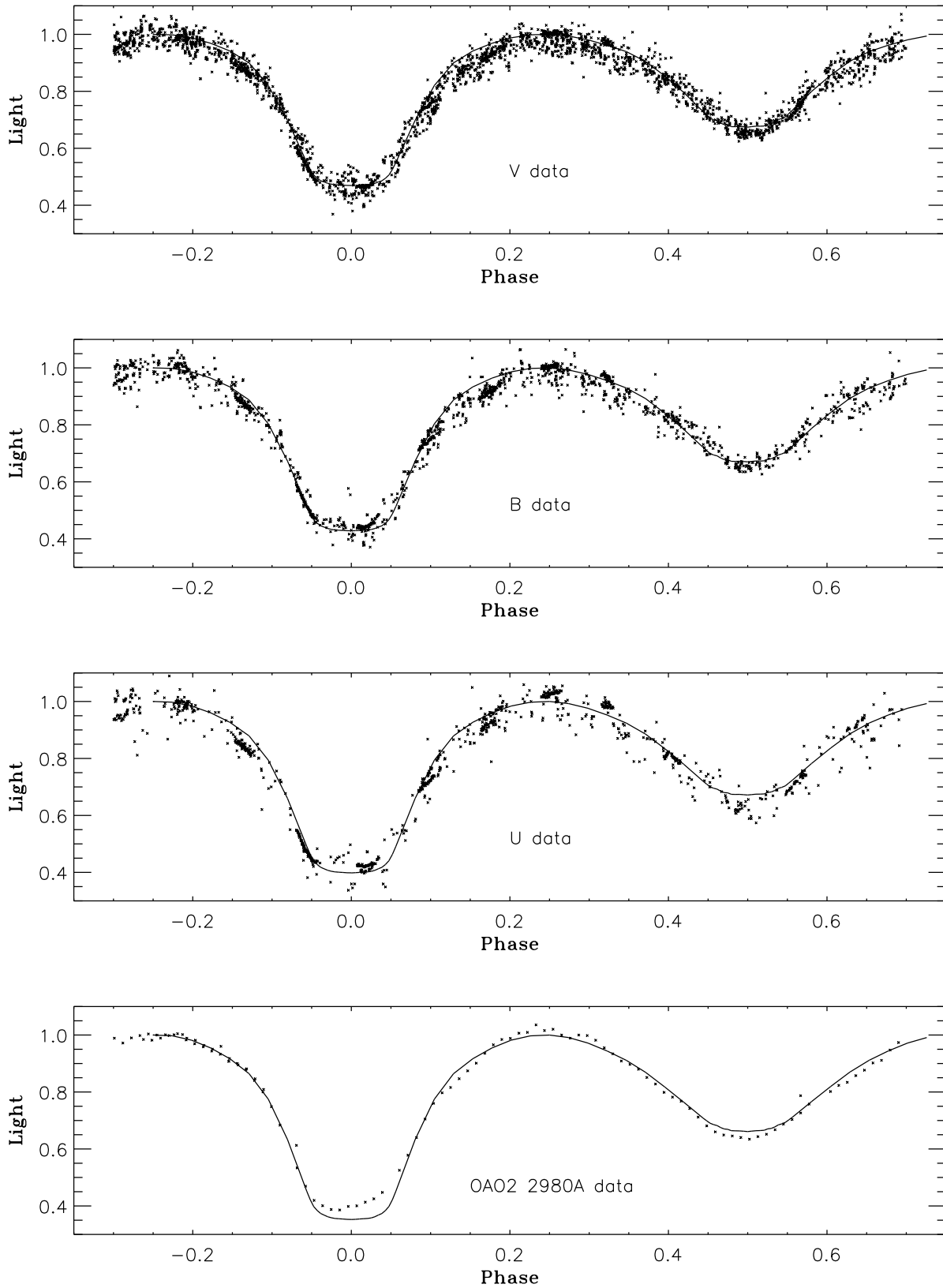


FIG. 4.—Comparison of theoretical and observed light curves on the alternative (hot rim) model. This model avoids the defect of Fig. 1 and fits the observed light curves well. The comparison with the *OAO 2* data shows the beginning of a discrepancy in the UV wavelength region.

This paper makes no attempt to represent the 283 day light variation (Guinan 1989; Van Hamme, Wilson, & Guinan 1996; HMB96) or to propose an explanation for it.

A projection view of the system at midprimary minimum

is in Figure 6. As with Figure 2, the rim has been represented with nine division circles on the toroidal boundary. The topmost division circle is below the observer's horizon. Note that the line of sight tangent to the top rim just grazes

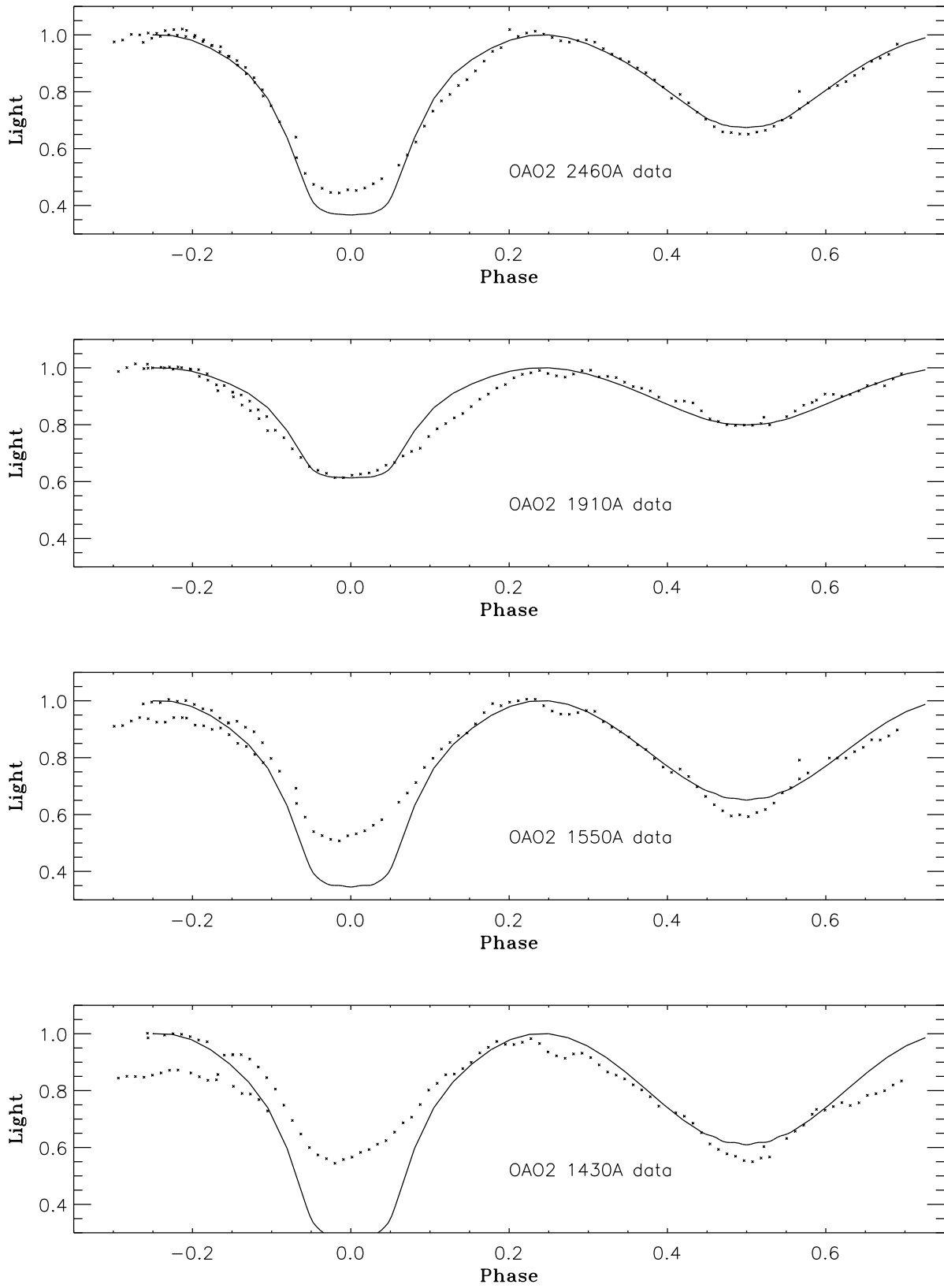


FIG. 5.—Comparison of theoretical and observed light curves on the alternative (hot rim) model, extending to shorter wavelengths than Fig. 4. Two effects are apparent. First, there is an increasing discrepancy between theory and observation in going to shorter wavelengths. The discrepancy arises from too little high- $T_{\text{eff}}$  radiation in the system model. Second, the amplitude of observed light variation reaches a minimum at 1910 Å. See text for details on both effects.

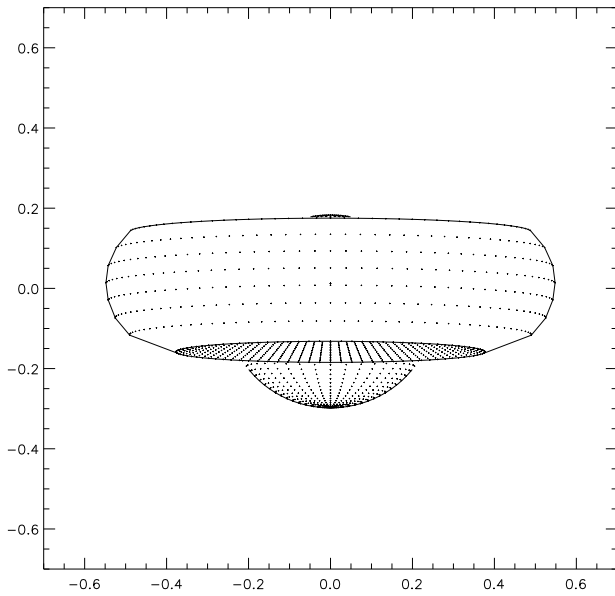


FIG. 6.—View of the alternative (hot rim) model projected on the plane of the sky at orbital phase 0.0. Note the visibility of the extreme upper polar region of the primary component. See text for a discussion of the rim visibility.

the polar region of the primary component.

In addition to the large rim  $T_{\text{eff}}$ , discussed below, this model has the undesirable feature of extending slightly beyond the boundary of the Roche lobe, at least for the equatorial part of the accretion disk rim, but by an amount less than the WL model.

#### 6. SPECTRUM SYNTHESIS ON THE ALTERNATIVE MODEL

Since our software self-consistently calculates both synthetic light curves and synthetic spectra, it is of interest to see how well the alternative model represents the *IUE* spectra. Figure 7 presents that comparison. The absence of a necessary high- $T_{\text{eff}}$  component is apparent. In the alternative model there are three sources of radiation: the primary

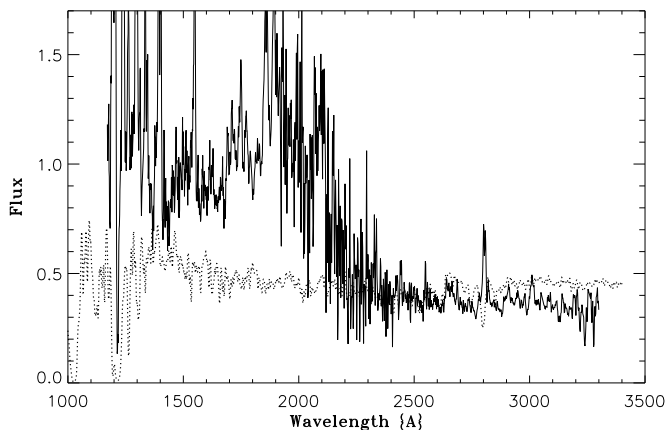


FIG. 7.—Comparison of the observed *IUE* spectrum during primary minimum at the orbital phase of Fig. 2 and a synthetic spectrum on the alternative (hot rim) model. The continuous line marks the *IUE* spectrum. The dotted line represents the synthetic spectrum. The extreme discrepancy with the observed continuum is apparent. As with the light curves of Fig. 5, the continuum discrepancy arises from too little high- $T_{\text{eff}}$  radiation in the model. The greater prominence of the emission lines, as compared with Fig. 3, arises from a different scaling factor for the observed spectrum. See text for discussion.

component, the accretion disk face, and the accretion disk rim. The face contribution is small. Its projected area is much less than that of the rim, the visible area is strongly limb-darkened because of the large angle between the surface normal and the line of sight, and only the lower temperature outer rings of the accretion disk face are visible. The theoretical continuum gradient in Figure 7 is consistent with the  $T_{\text{eff}}$  values for the primary component, Table 2, and the rim, Table 3.

Extensive sampling of parameter space convinces us that no alternative combination of adjustable system parameters, within the context of standard accretion disk theory, can produce synthetic light curves and synthetic spectra that satisfactorily fit the observed data. We emphasize that the BINSYN calculation of both the synthetic light curves and the synthetic spectra are on a self-consistent basis from a single physical model and that both the synthetic spectra and the synthetic light curves are essential parts of the analysis. The calculations presented here represent the first time that a standard model accretion disk has been applied in an analysis of  $\beta$  Lyrae.

#### 7. WHERE IS THE RIM BRIGHT SPOT?

The  $\dot{M}$  value from period change data (HS) is much larger than is common for cataclysmic variable systems, and so might be expected to produce a rim bright spot. Inspection of the light curves of Figure 4 and Figure 5 reveals no obvious photometric bright spot signature.

We have incorporated a solution of the equations for the transfer stream trajectory (Lubow & Shu 1975) in the BINSYN suite. Figure 8 displays an orbital plane view of the system, including the accretion disk for the HP model. The mass transfer stream trajectory is visible, including the location of its impact on the accretion disk rim, at an azimuth of  $6^\circ$  as seen from the center of the gainer. Analogy with CV systems leads to the expectation that a bright spot, extending downstream from the impact site, should brighten the egress branch of primary minimum or the ingress of

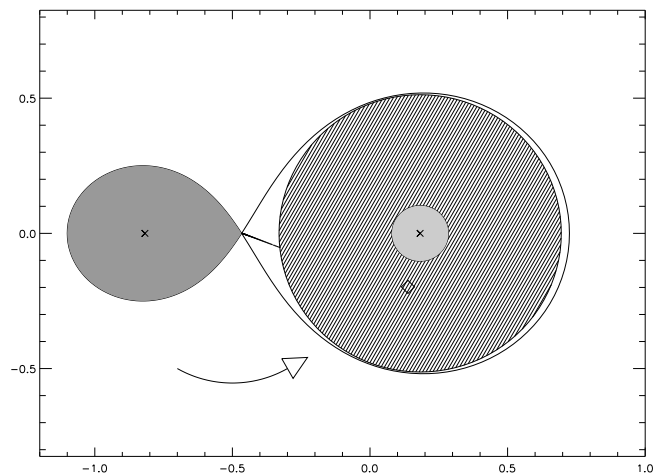


FIG. 8.—Orbital plane view of the HP model. The plot shows the trajectory of the mass transfer stream, on the Lubow-Shu theory. The radius of the accretion disk in its equatorial plane is  $30.0 R_{\odot}$ . Note that it nearly fills the Roche lobe. The accretion disk rim has the shape of a half-toroid with a cross-sectional radius of  $6.0 R_{\odot}$ . Thus, the inner edge of the half-toroid has a radius of  $24.0 R_{\odot}$ . The separation of centers of the components is  $58.35 R_{\odot}$ . A diamond marks the position calculated by Harmanec for the localized region of strong H $\alpha$  absorption. The arrow indicates the direction of orbital motion.

the secondary minimum and produce strong asymmetry in both minima. The Figure 5 light curves show that, if anything, the system is anomalously faint during late egress from the primary minimum, although the quality of photometric data does not allow us to draw definite conclusions. Close examination of Figure 4 shows that the same anomaly may be present in the  $V$ ,  $B$ , and  $U$  light curves. (Note that, in the case of dwarf novae systems, primary minimum corresponds to eclipse of the accretion disk object, and the bright spot is visible during the ingress to primary minimum.)

We suggest that the deposited kinetic energy is liberated at large optical depth (Olson 1980; Warner 1995, p. 39). The absence of a bright spot in the  $\beta$  Lyrae system parallels the same effect found in the hot Algol system MR Cygni (Linnell et al. 1998). We further propose that any emission from the stream-disk interaction is spread around a large portion of the rim. The deposited energy may produce a local vertical expansion of the rim and so lead to additional obscuration, explaining the asymmetry of primary minimum. This suggestion parallels the “dipping sources” in low-mass X-ray binaries (Livio 1993).

HMB96 provide evidence for jetlike structures associated with the secondary component. That paper also calculates a position for the center of a localized region within which the bulk of the  $H\alpha$  absorption takes place and argues that the jet may be associated with deflection of at least part of the mass transfer stream out of the orbital plane. That position is marked by a diamond on Figure 8. It lies directly on the extended theoretical trajectory of the mass transfer stream. Recently, Hoffman, Nordsieck, & Fox (1998, hereafter HNF) have presented extensive spectropolarimetric data for  $\beta$  Lyrae. They find that there is an asymmetry in the degree of polarization and polarized flux curves, with more negative values before secondary eclipse, roughly in the same orbital phase for which HMB96 find enhanced  $H\alpha$  absorption, which they also interpret as a signature of an extended light-scattering region above the accretion disk.

## 8. DISCUSSION: WHERE DO WE GO FROM HERE?

Shore & King (1986) suggest that a turbulent boundary layer in systems like  $\beta$  Lyrae might be the source of radiation leading to the ultraviolet excess. Our simple boundary layer model in BINSYN uses the innermost face ring to radiate the calculated boundary layer luminosity, assuming the central star rotates synchronously. This boundary layer is hidden on both the HP and alternative models. Regev (1991) provides an improved prescription for calculating the boundary layer and shows that the boundary layer may swell both perpendicular to and in the orbital plane. See also Kley (1991), Narayan & Popham (1994), and Popham (1997). Even if the radial swelling becomes as large as the radius of the gainer, it would be too small to produce the required observational effect and would have the wrong spectral characteristics. The BINSYN boundary layer model assigns the boundary layer radiating area (standard model, FKR, § 6) to an equal area for the two surfaces of the innermost accretion disk ring. This area, together with the energy to be dissipated, assuming synchronous rotation of the central star, produces a boundary layer  $T_{\text{eff}}$  of 21,000 K. If the energy were spread over a swollen surface, the  $T_{\text{eff}}$  would be smaller and would not provide the requisite high color temperature. Our discussion of the HP model shows that the source of the high- $T_{\text{eff}}$  radiation must extend in

radius by a large fraction of the accretion disk radius, a requirement inconsistent with the Shore & King (1986) proposal. If the central star is rotating near breakup (HP), the boundary layer luminosity is small. Drew (1997, hereafter DR) points out that the boundary layer now is considered to be a minor contributor to the total luminosity of CV systems. Godon (1997, and references therein) shows that theoretical boundary layer temperatures, with detailed numerical modeling, are much lower than originally expected. We believe these considerations exclude the boundary layer as the source of high- $T_{\text{eff}}$  radiation in  $\beta$  Lyrae.

Let us recapitulate the requirements for the high- $T_{\text{eff}}$  source, restricting the physical framework to a physically plausible addition to the standard model accretion disk. (1) It must extend outward from the center of the accretion disk by about  $\frac{2}{3}$  of the accretion disk radius. This requirement arises from the observed width of secondary minimum. (2) It must be more or less symmetrical about the center of the accretion disk, again from the observed symmetry of secondary minimum. (3) It must have a color temperature greater than that of the primary, to produce the observed increasing depth of secondary minimum toward shorter wavelengths, but it must have a smaller surface brightness in  $V$  and  $B$ , to preserve the relative depths of primary and secondary eclipse in those spectral bands. (4) It appears to be a continuous spectrum, not a series of emission lines contributing radiation in restricted wavelength ranges. Requirements (3) and (4) exclude a stellar photosphere of dimensions to satisfy the size restriction of point (1) but can be satisfied by a diffuse source. A source of high color temperature radiation is available in the central star, and possibly also in the inner disk, hidden from direct view as shown in our discussion of the HP model.

To provide the high- $T_{\text{eff}}$  source, we propose the existence of a light-scattering region, located above and below the orbital plane. The putative scattering region may consist partly of the jets discussed by HMB96 and HNF, but may also be other more or less axially symmetric material—as required by the nearly symmetric secondary minimum. HMB96 finds that the jets appear to be offset from the center of the accretion disk. Our light-scattering-region model is consistent with the “disk-disk” case in the HNF discussion.

The light-scattering source may be somewhat related to disk “coronae” of the CV systems, discussed by many authors (Liang & Price 1977; Galeev, Rosner, & Vaina 1979; Heyvaerts 1991; Meyer & Meyer-Hofmeister 1994; White 1997; Liu, Meyer, & Meyer-Hofmeister 1997). Cheng & Lin (1992) adopt a hot corona in their analysis of SS Cygni. Knigge & Drew (1996) show that light scattering is important in their disk wind model.

MHD turbulence in accretion disks now is generally regarded as the source of viscous transport of angular momentum (Balbus & Hawley 1991; Pringle 1994; Vishniac & Brandenburg 1997; Brandenburg & Campbell 1997; Balbus & Hawley 1997). Representative numerical simulations are in Brandenburg et al. (1995), Stone et al. (1996), Balbus, Hawley, & Stone (1996), and Hawley & Balbus (1997).

The light-scattering source may include material in the wind expected to be associated with the massive secondary component (Mazzali et al. 1992). Wind from the accretion disk faces (DR) may also contribute to the scattering

medium. See the study of the accretion disk wind in UX Ursae Majoris by Knigge & Drew (1997). Hydrodynamical models of disk winds are in Pereyra, Kallman, & Blondin (1997). The scattered radiation, scattered into the line of sight, is the high- $T_{\text{eff}}$  continuum of the secondary component. Isophotes for scattered radiation would increase in surface brightness closer to the secondary component—a “streetlight in a fog” effect. In the most elementary model the scattering would be optically thin, in the sense that radiation scattered into the line of sight from a given volume element (voxel) would continue through the remaining scattering medium without further diminution in intensity. This model would permit a reduction in the radiation contribution from the rim from the alternative (hot rim) model discussed previously. This change in turn requires reduction in the assumed  $\mathcal{M}$ . The rim thickness then would shrink, possibly producing a disk model comparable to that of HP.

Livio (1997) argues that, in addition to an accretion disk threaded by a vertical magnetic field, the production of powerful jets requires the presence of an energy or wind source associated with the central object. The present  $\beta$  Lyrae model, with its massive central star, meets this requirement. HNF provide spectropolarimetric evidence supporting the presence of two oppositely directed jets perpendicular to the orbital plane and associated with the accretion disk component. Their evidence is consistent with the same conclusion by HMB96. These jets parallel similar structures in CVs (DR).

The asymmetry of the 8.6  $\mu\text{m}$  light curve (JL) is in the correct sense to arise from downstream emission. The greater depths of secondary minimum at wavelengths longward of 2.2  $\mu\text{m}$  indicate a higher brightness temperature for the secondary component, considered as a composite object, than for the primary component. JL argue that this effect can be explained by a plasma cloud around the secondary component. This interpretation is in exact accord with our proposal for a light-scattering corona around the secondary component.

Without explicit simulation we are unable to predict whether the putative light-scattering region can produce the requisite high- $T_{\text{eff}}$  contribution to the continuum spectrum and the associated photometric effects. Calculation of these effects will require an appreciable addition to BINSYN and will require a programming effort of substantial duration. We postpone this calculation to a future effort.

## 9. CONCLUSIONS

1. We have used the BINSYN suite to calculate both synthetic light curves and synthetic spectra for  $\beta$  Lyrae on a common, self-consistent physical basis. Two models, the HP model and an alternative model, have been used for the simulation. Neither model can successfully represent the available light curves or an *IUE* spectrum at orbital phase 0.0158, for which we calculated synthetic spectra. We argue that no combination of adjustable parameters for a standard model accretion disk, with fixed parameters set to agree with their values, deduced from independent analyses, can satisfactorily model the available observational data.

2. The simulation failure arises from the absence of a necessary source of high- $T_{\text{eff}}$  radiation in our model of the  $\beta$  Lyrae system. We show that a stellar photosphere cannot be the source of high- $T_{\text{eff}}$  radiation. Its surface brightness would be too high.

3. A turbulent boundary layer, suggested by Shore & King (1986), cannot explain the UV excess and light curves in the  $\beta$  Lyrae system. This follows from geometrical constraints.

4. To resolve this dilemma, we propose the existence of a light-scattering region above the accretion disk faces. The region scatters high- $T_{\text{eff}}$  radiation from the central star and the inner disk into the line of sight—a “streetlight in a fog” effect—and we suggest that it is the source of the missing high- $T_{\text{eff}}$  continuum radiation, which is needed to explain observed spectrum and the light curves. The expected wind from the massive gainer, as well as a wind from the accretion disk, may contribute to the light scattering. The scattering region is likely separate from the source of strong emission lines, but may be closely related to the jets proposed by HMB96 and HNF. We postpone development of a model that includes this light-scattering region to a future effort.

5. The light curves near 2000 Å show a greatly reduced amplitude of light variation. This feature can be represented by the presence of third light, as first shown by WL. Our third light values (§ 5) differ substantially from those found by WL. Hack (1974) and others have argued that this light comes from the concentration of emission lines near 2000 Å, the “emission bump.” Since third light represents a light source that is not eclipsed, the emission bump region must be larger than the projected area of the binary system proper.

6. We have calculated the trajectory of the mass transfer stream and the location of its impact on the accretion disk rim. The observed light curves provide no compelling photometric signature of a rim bright spot. We suggest that the release of stream kinetic energy within the rim occurs over a sufficiently large region and at sufficient optical depth to avoid production of a bright spot region.

7. The observed light curves show a slight primary minimum asymmetry in the sense that egress light falls below ingress light at symmetric orbital phases. If there were a rim bright spot, it would preferentially affect the egress phases, an effect opposite to that observed. We speculate that the impact stream causes the downstream rim region to swell vertically, obscuring the system light sources behind it and producing the extra light loss.

A. P. L. has been partially supported by NASA grant NAG 5-3484 to Michigan State University, and P. H. was partly supported from the project K1-003-601/4 Astrophysics of Nonstationary Stars of the Academy of Sciences of the Czech Republic. We thank Jennifer Hoffman and Bob Wilson for making a number of comments on an initial version of this paper. The use of the computerized bibliography from the Strasbourg Astronomical Data Centre is also gratefully acknowledged.

## REFERENCES

- Armitage, P. J., & Livio, M. 1996, *ApJ*, 470, 1024  
 ———, 1998, *ApJ*, 493, 898  
 Aydin, C., Brandi, E., Engin, S., Ferrer, O. E., Hack, M., Sahade, J., Solivilla, G., & Yilmaz, N. 1988, *A&A*, 193, 202  
 Balachandran, S., Lambert, D. L., & Tomkin, J. 1986, *MNRAS*, 219, 479  
 Balbus, S. A., & Hawley, J. F. 1991, *ApJ*, 376, 214  
 ———, 1997, in *ASP Conf. Ser. 121, Accretion Phenomena and Related Outflows*, IAU Colloq. 163, ed. D. T. Wickramasinghe, G. C. Bicknell, & L. Ferrario (San Francisco: ASP), 90  
 Balbus, S. A., Hawley, J. F., & Stone, J. M. 1996, *ApJ*, 467, 76

- Berghöfer, T. W., & Schmitt, J. H. M. M. 1994, *A&A*, 292, L5
- Blondin, J. M. 1997, *BAAS*, 29, 779
- Brandenburg, A., & Campbell, C. 1997, in *Accretion Disks—New Aspects*, ed. E. Meyer-Hofmeister & H. Spruit (Springer: Berlin), 109
- Brandenburg, A., Nordlund, A., Stein, R. F., & Torkelsson, U. 1995, *ApJ*, 446, 741
- Buser, R., & Kurucz, R. L. 1992, *A&A*, 264, 557
- Cheng, F. H., & Lin, D. N. C. 1992, *ApJ*, 389, 714
- De Greve, J. P., & Linnell, A. P. 1994, *A&A*, 291, 786
- Dobias, J. J., & Plavec, M. J. 1985, *AJ*, 90, 773
- Drew, J. E. 1997, in *ASP Conf. Ser. 121, Accretion Phenomena and Related Outflows*, IAU Colloq. 163, ed. D. T. Wickramasinghe, G. V. Bicknell, & L. Ferrario (San Francisco: ASP), 465 (DR)
- Frank, J., King, A., & Raine, D. 1992, *Accretion Power in Astrophysics* (Cambridge: Cambridge Univ. Press) (FKR)
- Galeev, A. A., Rosner, R., & Vaina, G. S. 1979, *ApJ*, 229, 318
- Godon, P. 1997, *ApJ*, 483, 882
- Guinan, E. F. 1989, *Space Sci. Rev.*, 50, 35
- Hack, M. 1974, *A&A*, 36, 321
- Hack, M., Hutchings, J. B., Kondo, Y., & McCluskey, G. E. 1977, *ApJS*, 34, 565
- Harmanec, P. 1988, *Bull. Astron. Inst. Czechoslovakia*, 39, 329
- . 1992, *A&A*, 266, 307
- Harmanec, P., & Scholz, G. 1993, *A&A*, 279, 131 (HS)
- Harmanec, P., et al. 1996, *A&A*, 312, 879 (HMB96)
- Hawley, J. F., & Balbus, S. A. 1997, in *ASP Conf. Ser. 121, Accretion Phenomena and Related Outflows*, IAU Colloq. 163, ed. D. T. Wickramasinghe, G. V. Bicknell, & L. Ferrario (San Francisco: ASP), 179
- Heyvaerts, J. 1991, in *Structure and Emission Properties of Accretion Disks*, ed. C. Bertout, S. Collin, J.-P. Lasota, & J. Tran Thanh Van (Singapore: Fong & Sons), 109
- Hirose, M., Osaki, Y., & Mineshige, S. 1991, *PASJ*, 43, 809
- Hoffman, J. L., Nordsieck, K. H., & Fox, G. K. 1998, *AJ*, 115, 1576 (HNF)
- Huang, S. 1963, *ApJ*, 138, 903
- Hubeny, I., Harmanec, P., & Shore, S. N. 1994, *A&A*, 289, 411 (HH)
- Hubeny, I., & Plavec, M. 1991, *AJ*, 102, 1156 (HP)
- Jameson, R. F., & Longmore, A. J. 1976, *MNRAS*, 174, 217 (JL)
- Kley, W. 1991, in *Structure and Emission Properties of Accretion Disks*, ed. C. Bertout, S. Collin, J.-P. Lasota, & J. Tran Thanh Van (Singapore: Fong & Sons), 323
- Knigge, C., & Drew, J. E. 1996, *MNRAS*, 281, 1352
- . 1997, *ApJ*, 486, 445
- Kondo, Y., McCluskey, G. E., Silvis, J. M. S., Polidan, R., McCluskey, C. P. S., & Eaton, J. 1994, *ApJ*, 421, 787
- Liang, E. P. T., & Price, R. H. 1977, *ApJ*, 218, 247
- Lin, D. N. C., & Pringle, J. E. 1976, in *IAU Symp. 73, Structure and Evolution of Close Binary Systems*, ed. P. Eggleton, S. Mitton, & J. Whelan (Dordrecht: Reidel), 237
- Linnell, A. P. 1981, *Ap&SS*, 76, 61
- . 1984, *ApJS*, 54, 17
- Linnell, A. P., Etzel, P. B., Hubeny, I., & Olson, E. C. 1998, *ApJ*, 494, 773
- Linnell, A. P., & Hubeny, I. 1996a, *ApJ*, 471, 958 (LH)
- Linnell, A. P., Hubeny, I., & Lacy, C. H. S. 1996b, *ApJ*, 459, 721
- Liu, B. F., Meyer, F., & Meyer-Hofmeister, E. 1997, *A&A*, 328, 247
- Livio, M. 1993, in *Accretion Disks in Compact Stellar Systems*, ed. C. Wheeler (Singapore: World Scientific), 243
- . 1997, in *ASP Conf. Ser. 121, Accretion Phenomena and Related Outflows*, IAU Colloq. 163, ed. D. T. Wickramasinghe, G. V. Bicknell, & L. Ferrario (San Francisco: ASP), 845
- Lubow, S. H., & Shu, F. H. 1975, *ApJ*, 198, 383
- Mazzali, P. A. 1987, *ApJS*, 65, 695
- Mazzali, P. A., Pauldrach, A. W. A., Puls, J., & Plavec, M. J. 1992, *A&A*, 254, 241
- Meyer, F., & Meyer-Hofmeister, E. 1994, *A&A*, 288, 175
- Narayan, R., & Popham, R. 1994, in *Theory of Accretion Disks 2*, ed. W. J. Duschl, J. Frank, F. Meyer, E. Meyer-Hofmeister, & W. M. Tscharnuter (Dordrecht: Kluwer), 293
- Olson, E. C. 1980, *ApJ*, 241, 257
- Osaki, Y., Hirose, M., & Ichikawa, S. 1993, in *Accretion Disks in Compact Stellar Systems*, ed. J. C. Wheeler (Singapore: World Scientific), 272
- Paczynski, B. 1977, *ApJ*, 216, 822
- Pereyra, N. A., Kallman, T. R., & Blondin, J. M. 1997, *ApJ*, 477, 368
- Perryman, M. A. C., Hög, E., Kovalevsky, J., Lindgren, L., Turon, C. 1997, *ESA SP-1200, The Hipparcos and Tycho Catalogs*
- Polidan, R. S. 1989, *Space Sci. Rev.*, 50, 85
- Popham, R. 1997, in *ASP Conf. Ser. 121, Accretion Phenomena and Related Outflows*, IAU Colloq. 163, ed. D. T. Wickramasinghe, G. V. Bicknell, & L. Ferrario (San Francisco: ASP), 230
- Pringle, J. E. 1994, in *Theory of Accretion Disks 2*, ed. W. J. Duschl, J. Frank, F. Meyer, E. Meyer-Hofmeister, & W. M. Tscharnuter (Dordrecht: Kluwer), 357
- Regev, O. 1991, in *Structure and Emission Properties of Accretion Disks*, ed. C. Bertout, S. Collin, J.-P. Lasota, & J. Tran Thanh Van (Singapore: Fong & Sons), 311
- Rózycka, M., & Schwarzenberg-Czerny, A. 1987, *Acta Astron.*, 37, 141
- Sahade, J. 1980, *Space Sci. Rev.*, 26, 349
- Shore, S. N., & King, A. R. 1986, *A&A*, 154, 263
- Stone, J. M., Hawley, J. F., Gammie, C. F., & Balbus, S. A. 1996, *ApJ*, 463, 656
- Van Hamme, W., Wilson, R. E., & Guinan, E. F. 1996, *AJ*, 110, 1350
- Viotti, R. 1976, *MNRAS*, 177, 617
- Vishniac, E. T., & Brandenburg, A. 1997, *ApJ*, 475, 263
- Wade, R. A., & Rucinski, S. M. 1985, *A&AS*, 60, 471
- Warner, B. 1995, *Cataclysmic Variable Stars* (Cambridge: Cambridge Univ. Press)
- White, N. E. 1997, in *ASP Conf. Ser. 121, Accretion Phenomena and Related Outflows*, IAU Colloq. 163, ed. D. T. Wickramasinghe, G. V. Bicknell, & L. Ferrario (San Francisco: ASP), 142
- Wilson, R. E. 1974, *ApJ*, 189, 319
- . 1981, *ApJ*, 251, 246
- Wilson, R. E., & Devinney, E. J. 1971, *ApJ*, 166, 605
- Wilson, R. E., & Lapasset, E. 1981, *A&A*, 95, 328 (WL)
- Zhang, E.-H., & Robinson, E. L. 1987, *ApJ*, 321, 813
- Zhang, E.-H., Robinson, E. L., & Nather, R. E. 1986, *ApJ*, 305, 740
- Zola, S. 1996, *A&A*, 308, 785
- Zola, S., Hall, D. S., & Henry, G. W. 1994, *A&A*, 285, 531